Synthesis of Ag_2O/TiO_2 and CuO/TiO_2 composites for the photocatalytical mineralization of iopromide in water under UV and visible light irradiation

Durán-Álvarez J.C.[1,*], Hernàndez-Morales V.A. [1], Castıllón F. [2], And Zanella R.[1]

[1]Centro de Ciencias Aplicadas y Desarrollo Tecnológico, Universidad Nacional Autónoma de México, Circuito Exterior S/N, Ciudad Universitaria, P.O. BOX 70-186, Cd Mx, 04510, México

[2]Centro de Nanociencias y Nanotecnología, Universidad Nacional Autónoma de México, Km 107 Carretera Tijuana-Ensenada, P.O. BOX 14, 22800, Ensenada, Baja California, México

*corresponding author: J.C. Duràn-Álvarez, Tel +52 55 56228602 ext 1301

e-mail: carlos.duran@ccadet.unam.mx

Abstract X-ray contrast media are emerging contaminants in water. These contaminants are recalcitrant in conventional treatment systems, although advanced oxidation processes, such as heterogeneous photocatalysis, are able to achieve high degradation rates using UV and visible light. In this work, nanoparticles of metal oxides (Ag_2O and CuO) were deposited on TiO_2 in order to increase the photocatalytic mineralization of iopromide using either UV or visible light. The synthesized photocatalysts were characterized by XRD, TEM, XPS, DRS and ICP-OES. Photocatalytic activity was determined using surface modified P25 TiO_2 with different loadings of Ag_2O and CuO nanoparticles. Surface modified TiO_2 showed higher activity compared with photolysis and bare TiO_2. Mineralization rates of 85 and 60% resulted when 2% wt. Ag_2O/TiO_2 and 0.5% wt. CuO/TiO_2, respectively, were tested under UV-C light irradiation. When UVA-visible light was used in irradiation tests, 2% wt. Ag_2O/TiO_2 displayed higher mineralization rate (60%) than the 0.5% wt. CuO/TiO_2 material (<10%). When photocatalysis tests were performed using tap water, mineralization was decreased up to 20% after 5 h of UVA-visible light irradiation when the 2% wt. Ag_2O/TiO_2 was used, while 0.5% wt. CuO/TiO_2 showed negligible activity. Even when mineralization rate was low in tap water, the complete degradation of iopromide molecule was achieved for both materials and BOD increased at the end of irradiation tests. Some of the intermediates were identified by LC-MS/MS, these compounds showed no acute toxicity in bioluminescence tests using *V. fischeri*.

Keywords: emerging pollutants; photocatalysis; X-ray contrast media

1. Introduction

Iodinated X-ray contrast media (ICM) are acknowledged as emerging contaminants in water (Seitz *et al*., 2006). This group is one of the most used pharmaceutical compounds worldwide, just after antibiotics and anti-inflammatory drugs (Daughton, 2004). By the early 2000s,

it was estimated that 3,500 Tons per annum of ICM were used in developed countries (Pérez and Barceló, 2007). Given that ICM have no biological interaction within human body, most of the applied dose pass through the human body and is fully excreted by urine within one day; no glucoronides or sulfate conjugated are formed (Bourin *et al*., 1997). As happens for most emerging pollutants, wastewater is the main route of the ICM to get into environment. The highest concentrations of ICM have been reported in hospital wastewater (in the range of mg/L to µg/L) (Weissbrodt *et al*., 2009), followed by municipal wastewater. Due to the high polarity and inertness of ICM, very low removal rates in conventional wastewater treatment systems have been systematically reported (Kormos *et al*., 2011). Because of this, concentrations of ICM in effluents of wastewater treatment plants can be as high as those found in influents, and thus this kind of contaminants can reach surface water and soils. Concentrations of ICM in surface waters is reported within the µg/L-ng/L range (Kalsch, 1999; Carballa *et al*., 2004; Seitz *et al*., 2006; Haiß and Kümmerer, 2006; Pérez and Barceló, 2007; Schulz *et al*., 2008; Kormos *et al*., 2010; Kormos *et al*., 2011). ICM displaying high water solubility can leachate through soil toward the aquifer, which has resulted in the occurrence of these compounds at trace levels in drinking water sources (Putschew *et al*., 2000; Drewes *et al*., 2001; Schittko *et al*., 2004). Even with the continuous occurrence of ICM in water bodies and soil, no harmful effects have been reported in exposed aquatic or soil organisms (Steger-Hartmann *et al*., 2002; Seitz *et al*., 2006; Crane *et al*., 2006); moreover, it is unclear the risks that ICM and their by-products may pose to ecosystem. Nevertheless, precautionary principle compels that under lack of knowledge on the toxic effects caused by ICM, these pollutants should be removed from wastewater and drinking water in order to avoid unexpected effects in the long term.

Membrane processes are able to achieve removal rates of up to 90% for most ICM (Clara *et al*., 2005; Hapeshi *et al*., 2013; Eversloh *et al*., 2014); however, mineralization rates are low, and both the target compounds and their by-products (especially when bioprocesses are involved) are

transferred from the water phase to the sludge. Advanced oxidation processes, such as UV photolysis, ozonation and Fenton reaction have also shown high degradation rates of ICM, although low mineralization has been reported so far (Ternes *et al*., 2003; Fitzke and Geissen, 2007; Chu *et al*., 2011; Zhao *et al*., 2014). In order to guarantee harmless effluents, either the complete mineralization of the pollutants or the increase of biodegradability of effluents should be achieved. In this regard, heterogeneous photocatalysis using UV or UV-visible light has shown high mineralization rates of ICM in water.

Previous studies report the mineralization of some ICM using TiO_2 as photocatalyst (Sugihara *et al*., 2013; Azerrad *et al*., 2014). This semiconductor is widely used in water treatment systems since its low cost, inocuity and high performance; however, due to its high band gap value (E_g = 3.2 eV), such efficiency is only possible when UV light (λ < 380 nm) is used (Hashimoto *et al*., 2005). Due to this limitation, many efforts have been performed to modify the E_g of TiO_2 and thus increase its photoactivity within the visible light spectrum. Doping with non-metal atoms, sensitization with azo dyes and formation of heterostructures using metallic and metal oxide nanoparticles have been the most commonly used approaches (Chong *et al*., 2010). In our previous works, modification of TiO_2 by deposition of metallic nanoparticles (Au, Ag, Cu, Ni) resulted in the increment of the photocatalytic removal of antibiotics in pure water (Oros-Ruíz *et al*., 2013; Durán-Álvarez *et al*., 2016). Metallic Ag, Cu and Ni nanoparticles are oxidized during the photocatalytic process, resulting in the formation of metal oxide (M_XO) nanoparticles. However, the M_XO/TiO_2 heterostructures resulted as photoactive as the M/TiO_2 structures. Moreover, in some cases, surface modified TiO_2 with metal oxide nanoparticles have shown higher photocatalytic activity for the removal of organic pollutant in water and hydrogen production compared with M/TiO_2 and unmodified TiO_2 materials (Oros-Ruíz *et al*., 2015). In this work, Ag_2O and CuO nanoparticles were deposited on TiO_2 and tested for the photocatalytic degradation of the ICM compound iopromide. Mineralization of this emerging pollutant was tested using either UV (254 nm) or UVA-visible light (380-800 nm) in pure and tap water. Some intermediate were identified and their toxicity was determined by decay of *V. fischeri* bioluminescence.

2. Materials and methods

2.1. Synthesis and characterization of the materials

Degussa P25 TiO_2 (specific surface area of 52 m^2/g, 70% anatase and 30% rutile) was used as support for deposition of either Ag_2O or CuO nanoparticles. Supporting of metal oxide nanoparticles was performed by the deposition-precipitation method. In brief, the precise amount of the Ag_2O and CuO precursors, $AgNO_3$ and $Cu(NO_3)_3$·$2.5H_2O$ respectively, was dissolved in distilled water; then, 1 g of P25 TiO_2 was added and the suspension was thoroughly stirred. The pH of the suspension was < 4. Stirring was provided for some minutes in order to stabilize the suspension; then, a basifying agent was added in order to precipitate the metallic precursor. For the precipitation of Ag_2O, 0.05 M NaOH solution was dropwise added until

the pH value was raised to 9.0. When the precipitation of CuO was pursued, urea was used as precipitation agent. The amount of urea used was established as the Cu:urea molar ratio of 1:100. The suspensions were stirred at 80ºC for 4 h and 16 h in order to complete the deposition of Ag_2O and CuO, respectively. After this time, the solid phase was recovered by centrifugation at 10500 rpm for 5 min; then, 4 washing cycles were performed using 100 mL of distilled water in each single cycle. Once washing cycles were over, the materials were dried at 80 ºC for 2 h under vacuum conditions. Lastly, thermal treatment at 150 and 350ºC was supplied in order to obtain Ag_2O and CuO nanoparticles, respectively. The heating cycle was performed for 3 h in air atmosphere, setting a temperature ramp of 2ºC/min from 25ºC. After thermal treatment, all the materials were stored under dry and dark conditions. The loadings of Ag_2O and CuO nanoparticles supported on TiO_2 were set as 0.25; 0.5; 1.0; 2.0 and 3.0 wt. % for both metals.

The crystallographic phase of metal oxide nanoparticles was determined by the X-ray diffraction technique. The form and size of the metal oxide nanoparticles was determined by TEM analysis. Specific surface area of the modified materials was elucidated by the N_2 absorption method. The light absorption of each material was determined by UV-vis spectrophotometry. The chemical composition of the materials before and after photocatalysis tests was determined by XPS and ICP-OES analyses.

2.2. Photocatalysis tests

The photocatalytic mineralization of iopromide was performed in batch tests under either UV or UVA-vis irradiation. In these experiments, the photocatalytyc activity of unmodified materials (P25 TiO_2, CuO and Ag_2O) and the surface modified TiO_2 with different loadings of Ag_2O and CuO nanoparticles was tested; photolysis experiments were also performed for comparative proposes. In each experiment, 250 mL of a 30 mg/L iopromide solution in pure water were mixed with 125 mg of each photocatalyst. The suspensions were put in a glass reactor under vigorous magnetic stirring. Dark conditions were maintained for 30 min in order to achieve the adsorption equilibrium, and then the light source was turned on. The light source for UV and UVA-visible light were a low pressure Hg lamp (λ = 254 nm) and a 150 W Xenon lamp (λ = 380-800 nm), respectively. The lamp was immersed into the suspension in order to guarantee the highest photonic efficiency. The temperature of each reaction was maintained at 25ºC, using a water bath. In all the irradiation experiments, air was bubbled at 100 mL/min in order to keep the oxygen saturation in water. Irradiation tests were carried out for 5 h, and 8 mL samples were withdrawn from the reactor with a syringe throughout the experiment. At the end of irradiation tests, the photocatalyst was recovered from the suspension by centrifugation at 10500 rpm for 5 min; then, it was dried at 80ºC for 2.5 h. The recovered solid material was used in three consecutive reaction cycles in order to assess its photo stability. Lastly, in order to evaluate the impact of the dissolved components in water (matrix effect), photocatalysis experiments were carried out in tap water

under the reaction conditions described above, and using the material with the best photocatalytic performance in pure water.

2.3. Analytical methods

All the water samples taken in irradiation experiments were passed through 0.45 μm nylon membranes and analyzed in a TOC-L Shimadzu equipment in order to determine the mineralization rate of iopromide. The elucidation of degradation rate of iopomide and the identification of some intermediates was determined by LC-MS/MS analysis. Separation was done using a LC–ESI–MS/MS Agilent Technologies 6400 series equipment, with a C18 Eclipse Plus (2.1 mm × 150 mm × 3.5 μm) column. 0.1% formic acid and acetonitrile were used isocartically at 0.4 mL/min. Electrospray was used to ionize the analytes and mass spectroscopy analysis was performed using the positive polarity mode. For the fragmentation of the analytes, cone voltage was maintained at 60 V; the drying gas (nitrogen) was supplied using a flow rate of 13 L/min and 350°C; the voltage of the capillary was set at 3000 V; the collision cell voltage was 16 V.

2.4. Toxicity tests

In order to determine the potential harmful effects caused by intermediates, toxicity tests were performed in water samples taken throughout the photocatalysis tests. As a first step, chemical oxygen demand was determined at the beginning and at the end of irradiation experiments under UVA-visible light, in order to determine changes in the biodegradability of effluent.

Acute toxicity was assessed in water samples taken upon 60, 90, 120 and 300 min of UVA-vis irradiation. Toxicity was determined via inhibition of the bioluminescence of the marine bacteria $V.$ $fischeri$, using a LUMIStox 300 kit (HACH LANGE), and following the standard methodology ISO 11348–3.

3. Results and discussion

3.1. Characterization of the materials

XRD confirmed the typical composition of the P25 TiO_2 material, namely 70% anatase and 30% rutile. When the surface modified TiO_2 materials were analyzed, cubic and monoclinic crystallographic phases of Ag_2O and CuO were distinguished, respectively. Such phases have been commonly reported in binary heterostructures with TiO_2. More importantly, these crystallographic phases display relevant photocatalytic activity (Qin et $al.$, 2011; Wang et $al.$, 2011). The average size of the metal oxides nanoparticles deposited on P25 TiO_2 was determined by TEM analysis. Through the analysis of at least 500 particles in 30 micrographies, it was determined that the mean size of Ag_2O nanoparticles was 5 nm, while for CuO nanoparticles, size was in the range of 4-8 nm. No increment in the average nanoparticle size was observed when the loading of metal oxides was increased. Tiny and well dispersed nanoparticles of Ag_2O and CuO semiconductors are suitable to promote the photocatalysis

process under visible light irradiation, due to their low band gap value (Barreca et $al.$, 2009; Zhou et $al.$, 2010). Specific surface area of P25 TiO_2 was not significantly modified upon deposition of metal oxide nanoparticles, which may be attributed to the low specific surface area, the shape and the heterogeneous dispersion of the Ag_2O and CuO nanoparticles. XP spectra showed that Ag and Cu deposited on TiO_2 were majorly in their oxidized form, as Ag^{+1} and Cu^{+2}. However, some other species were also occurring at trace levels within the nanoparticles, namely AgO and metallic silver in the case of Ag_2O, and Cu_2O and metallic cupper in the case of CuO nanoparticles. It has been previously reported that photocatalytic activity of metal oxides can be increased when mixed chemical species are present within the nanoparticles. In the case of Ag_2O nanoparticles, the occurrence of AgO can be explained as an intermediate in the reduction of Ag_2O into metallic silver (Kerkez and Boz, 2014). In order to determine the actual loading of metal oxides deposited on TiO_2, and thus the efficiency of the synthesis method based on deposition-precipitation, elemental analysis by ICP-OES was carried out. Deposition of Ag_2O nanoparticles was less effective compared with that of CuO nanoparticles. This may be explained by the use of NaOH as basifying agent, which results in lower and uncontrolled deposition rates of Ag. NaOH was used for Ag deposition since urea can form soluble species, hindering Ag precipitation. The light absorption spectra of the modified materials showed no modification in band gap energy (E_g) value of TiO_2 upon deposition of metal oxides. This was expected given that no interband states are formed by surface modification of semiconductors, as occurs when doping with non-metal atoms is performed (DiValentin and Pacchioni, 2013) Even when E_g value was not modified by deposition of metal oxide nanoparticles, absorption bands were observed in the visible light spectrum, corresponding to Ag_2O (λ= 480 nm) and CuO (λ= 600 nm), and indicating that the semiconductor nanoparticles deposited on TiO_2 may display photocatalytic activity under visible light irradiation

3.2. Photocatalytic mineralization of iopromide

3.2.1. Mineralization under UV light irradiation

Mineralization of iopromide by photolysis using a disinfection lamp (λ = 254 nm) resulted in less than 18% of TOC oxidation (Figure 1). This same behavior has been previously reported in earlier works (Borowska et $al.$, 2015). Mineralization of iopromide occurred due to the overlapping of the light absorption spectrum of the molecule (λ = 255 nm) and the emission of the UV-C light lamp. Given its high photostability, catalysis is necessary in order to achieve higher mineralization of this recalcitrant molecule. When P25 TiO_2 was used as photocatalyst, mineralization rate increased up to 36% upon 5 h or UV-C light irradiation, showing the efficiency of photocatalysis process. Irradiation tests using Ag_2O/TiO_2 materials showed an important improvement in mineralization rate, achieving 85% of TOC removal when the 2% wt. Ag_2O/TiO_2 material was used. The mineralization rate varied with the loading of Ag_2O
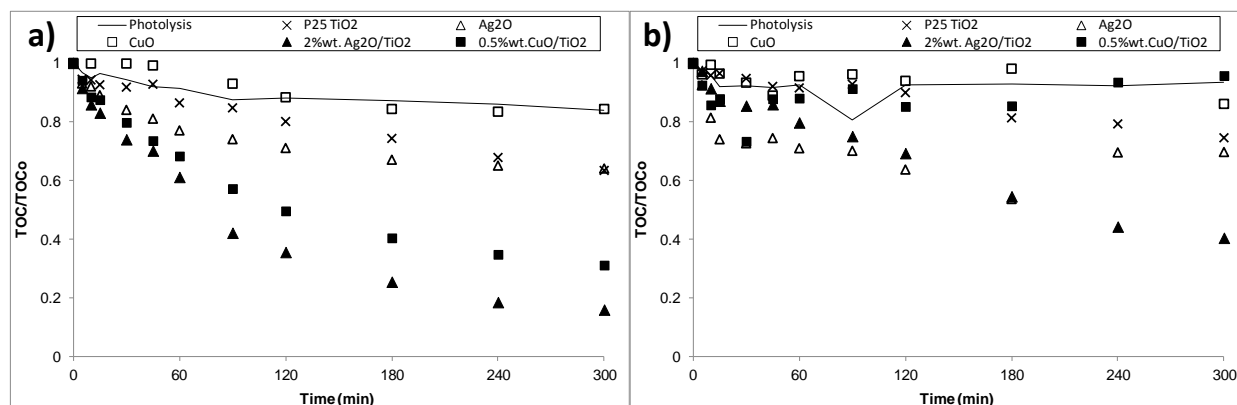
.

Figure 1. Photocatalytic mineralization of iopromide using a) UV and b) UVA-visible light

Table 1. Mineralization rate of iopromide in pure water using different loading of metal oxide nanoparticles under UV-C and UVA-visible light irradiation

Loading of metal oxide nanoparticles (% wt.)	UV-C light		UVA-visible light	
	Material			
	Ag_2O/TiO_2	CuO/TiO_2	Ag_2O/TiO_2	CuO/TiO_2
0	36		23	
0.25	64	61	52	3
0.5	78	69	54	8
1.0	80	56	58	6
2.0	85	45	60	4
3.0	75	53	55	4

nanoparticles (Table 1). The lowest activity was observed for 0.25% wt. Ag_2/TiO_2, then activity increased with the loading of Ag_2O nanoparticles, finding the optimal loading at 2% wt. Photocatalytic activity dropped when higher loadings were tested. For the CuO/TiO_2 materials, the optimal loading of the metal oxide nanoparticles was 0.5% wt.; using this material, mineralization rate was 70% upon 5 h of UV light irradiation. Similar to that observed for Ag_2O/TiO_2, increasing the CuO loading resulted in decay of the photocatalytic activity. The decrease in the mineralization rate by the increment of the nanoparticleloading can be explained by the saturation of TiO_2 surface, and suggests that both semiconductors are working together by transferring charge carries from one semiconductor to another, impeding the recombination of the hole/electron pairs, and increasing in turn the photoactivity (Li *et al*., 2008; Kerkez and Boz, 2015). Very low mineralization was observed when single Ag_2O and CuO nanoparticles were tested. Again, Ag_2O showed higher photocatalytic activity (36% of mineralization) than CuO (17% of mineralization). The low activity of the unmodified semiconductors may be related with: a) the very low surface area of the nanoparticles, which resulted in very low adsorption of iopromide; b) the high recombination rate of the electron-hole pair, which increased by the low particle size; and, c) the low photostability of the nanoparticles,

resulting in the occurrence of one single chemical specie (such as metallic Ag or CuO) instead of a combination of oxidation states, which tends to display higher photocatalytic activity. It is clear from these results the synergistic effect resulting from the mixture of two semiconductors.

3.2.2. Mineralization under UVA-visible irradiation

Photolysis of iopromide using a Xenon lamp resulted in mineralization rates lower than 5% upon 5 h of irradiation. This result is quite similar to that observed for the photocatalytic mineralization of fluoroquinoles under sunlight irradiation (Durán-Álvarez *et al*., 2016).

Testing P25 TiO_2 resulted in mineralization rate of 23%, which is slightly lower than that achieved under UV-C light irradiation. Activity of TiO_2 under Xenon lamp irradiation is explained by the UVA light contained in the Xenon lamp spectrum, which is able to photo activate TiO_2 (absorption edge of TiO_2 = 380 nm).

Mineralization rate of iopromide obtained by surface modified TiO_2 resulted lower than that observed under UV-C light, which is explained by the lower photolytic mineralization of the molecule as well as the lower activity of the TiO_2 support. In the case of Ag_2O/TiO_2 materials, mineralization rate of 60% was achieved upon 5 h of irradiation (Figure 1b). Variations in the photocatalytic performance related with the loading of Ag_2O were minimal compared with that observed under UV-C light

irradiation (Table 1). Contrary to that observed for Ag_2O/TiO_2 material, mineralization rates achieved using the CuO/TiO_2 materials were negligible compared with those obtained under UV-C light irradiation. Mineralization rate obtained by the 0.5% wt. CuO/TiO_2 material resulted in 8% upon 5 h of irradiation. Mineralization rate decreased as CuO loading increased, up to 4% when the 3% wt. CuO/TiO_2 material was tested. Low mineralization rate of CuO/TiO_2 materials may be explained by the decreased activity of both semiconductors under UVA-visible light. When only CuO is photo activated, the transfer of charge carriers from one semiconductor to another stops, and recombination occurs. CuO nanoparticles are unable to perform photocatalysis because of the high recombination occurring within this semiconductor (Li et al., 2008). Such recombination is not that strong in the Ag_2O/TiO_2 materials due to the reduction of Ag_2O into Ag° by photo generated electrons, which hinders the recombination and maintain the hole free to oxidize the adsorbed iopromide. Mineralization rates obtained under UVA-visible light using Ag_2O and CuO nanoparticles (30 and 12%, respectively) were lower than that observed for unmodified TiO_2. Similar to that observed in UV-C light irradiation experiments, Ag_2O was photo reduced into Ag° (determined by XPS analysis) by the UVA-visible light, which resulted in the drop of the photoactivity. When Ag species within nanoparticles (AgO and Ag_2O) are reduced into Ag°, photocatalytic activity is reduced, as reported by Kerkez and Boz, 2015,

Reuse tests under UVA-visible light irradiation evidenced the low stability of the Ag_2O/TiO_2 material. Throughout reuse cycles, the color of the 2% wt. Ag_2O/TiO_2 material changed from pale brown to grey and again into brown, indicating the reduction and reoxidation of silver during the process. By the second reuse cycle, iopromide mineralization rate decayed up to 20%, and this efficiency was maintained in the third reaction cycle, suggesting the stabilization of the Ag_2O nanoparticles. XPS analysis of the reused catalyst showed lixiviation of Ag from the nanoparticles, which may explain the drop in the catalytic activity by the second reaction cycle. In the case of the 0.5% wt. CuO/TiO_2 material, high stability was observed throughout three reaction cycles; although photocatalytic activity was significantly low (Figure 2). In the light of

these results, it is clear that Ag_2O/TiO_2 was the best material even with its low stability.

3.3. Mineralization in tap water

Mineralization kinetics of iopromide in tap water under UVA-visible irradiation was lower than that observed in pure water. The photocatalytic mineralization of iopromide using the 2% wt. Ag_2O/TiO_2 and 0.5% wt. CuO/TiO_2 materials was higher (13 and 5%, respectively) than those observed in photolysis and TiO_2 photocatalysis tests (1 and 4%, respectively). The low mineralization rates of iopromide may be caused by matrix effect, in which, the occurrence of HCO_3^- and CO_3^{-2} ions impact in the photocatalytic performance by scavenging the $^•OH$ radicals in the semiconductor surface (Chong et al., 2010). Inorganic carbon in tap water samples was 7.2 mg/L compared with 0.3 mg/L observed in pure water. Even when mineralization was decreased, degradation was not affected by matrix effect. In fact, complete transformation of the organic molecule was achieved upon 45 min of UVA-visible irradiation, as shown by LC-MS/MS analysis.

3.4. By-products identification and toxicity tests

Given that complete mineralization was not achieved during photocatalysis tests, some of the intermediates were identified by LC-MS/MS. Photocatalytic degradation begins with amination of the aliphatic chains, followed by the dehalogenation of the benzene ring. Interestingly, the released iodide from the molecule may scavenge some of the free radicals produced on the photocatalyst materials, resulting in the decreasing of the photocatalytic activity.

BOD analysis showed the increment in the biodegradability in water samples from < 0.5 mg/L at the beginning of the reaction to 3 mg/L by the end of the photocatalytic reaction. Likewise, toxicity tests using V. fischeri showed no toxicity in samples taken throughout the photocatalytic reaction.
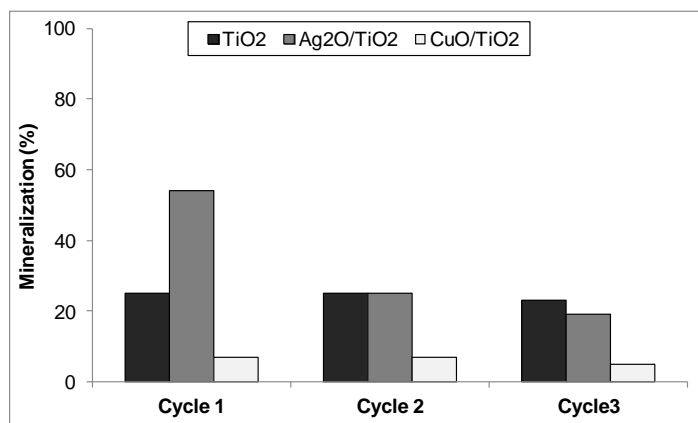
4.   Conclusions

Figure 2. Reusability of the photocatalyst materials upon 3 cycles using UVA-visible light

Ag$_2$O and CuO nanoparticles were successfully deposited on TiO$_2$ via deposition-precipitation method followed by thermal treatment in air. Binary composites are more efficient in the photocatalytic mineralization of iopromide in pure water under UV-C and UVA-visible light than photolysis and unmodified TiO$_2$. However, in tap water, matrix effect occurs and photocatalytic mineralization rates drop; still, the performance of modified materials is higher than that of bare TiO$_2$. Even when the complete mineralization of iopromide is achieved in photocatalysis process, by-products display no toxicity and higher biodegradability than the parent molecule. Ag$_2$O/TiO$_2$ can be used as a photocatalytic material to remove recalcitrant pollutants in water; however, further investigation should be done on the stabilization of silver nanoparticles.

References

Azerrad S.P., Gur-Reznik S., Heller-Grossman L., and Dosoretz C.G. (2014), Advanced oxidation of iodinated X-ray contrast media in reverse osmosis brines: the influence of quenching, *Water Research*, **62**, 107-116.

Barreca D., Fornasiero P., Gasparotto A., Gombac V., Maccato C., Montini T., and Tondello E. (2009), The potential of supported Cu$_2$O and CuO nanosystems in photocatalytic H$_2$ production, *ChemSusChem*, **2**, 230-233.

Borowska E., Felis E., and Żabczyński S. (2015), Degradation of iodinated contrast media in aquatic environment by means of UV, UV/TiO$_2$ process, and by activated sludge, *Water, Air, and Soil Pollution*, **226**, 151.

Bourin M., Jolliet P., and Ballereau F. (1997), An overview of the clinical pharmacokinetics of x-ray contrast media, *Clinical Pharmacokinetics*, **32**, 180-193.

Carballa M., Omil F., Lema J.M., Llompart M., García-Jares C., Rodríguez I., Gómez M., and Ternes T. (2004), Behavior of pharmaceuticals, cosmetics and hormones in a sewage treatment plant, *Water Research*, **38**, 2918-2926.

Chong M.N., Jin B., Chow C.W., and Saint C. (2010), Recent developments in photocatalytic water treatment technology: a review. *Water Research*, **44**, 2997-3027.

Chu W., Wang Y.R., and Leung H.F. (2011), Synergy of sulfate and hydroxyl radicals in UV/S$_2$O$_8^{2-}$/H$_2$O$_2$ oxidation of iodinated X-ray contrast medium iopromide, *Chemical Engineering Journal*, **178**, 154-160.

Clara M., Strenn B., Gans O., Martinez E., Kreuzinger N., and Kroiss H. (2005), Removal of selected pharmaceuticals, fragrances and endocrine disrupting compounds in a membrane bioreactor and conventional wastewater treatment plants, *Water Research*, **39**, 4797-4807.

Crane M., Watts C., and Boucard T. (2006), Chronic aquatic environmental risks from exposure to human pharmaceuticals, *Science of the Total Environment*, **367**, 23-41.

Daughton C.G. (2004), PPCPs in the environment: future research—beginning with the end always in mind. In: *Pharmaceuticals in the Environment*, 463-495. Springer Berlin Heidelberg.

Di Valentin C., and Pacchioni G. (2013), Trends in non-metal doping of anatase TiO$_2$: B, C, N and F, *Catalysis Today*, **206**, 12-18.

Doll T.E., and Frimmel F.H. (2004), Kinetic study of photocatalytic degradation of carbamazepine, clofibric acid, iomeprol and iopromide assisted by different TiO$_2$ materials—determination of intermediates and reaction pathways, *Water Research*, **38**, 955-964.

Drewes J.E., Fox P., and Jekel M. (2001), Occurrence of iodinated X-ray contrast media in domestic effluents and their fate during indirect potable reuse, *Journal of Environmental Science and Health, Part A*, **36**, 1633-1645.

Durán-Álvarez J.C., Avella E., Ramírez-Zamora, R.M., and Zanella R. (2016), Photocatalytic degradation of ciprofloxacin using mono-(Au, Ag and Cu) and bi-(Au–Ag and Au–Cu) metallic nanoparticles supported on TiO$_2$ under UV-C and simulated sunlight, *Catalysis Today*, **266**, 175-187.

Eversloh C.L., Henning N., Schulz M., Ternes T.A. (2014), Electrochemical treatment of iopromide under conditions of reverse osmosis concentrates–Elucidation of the degradation pathway, *Water Research*, **48**, 237-246.

Fitzke B., and Geißen, S.U. (2007), Sustainable removal of iodinated X-ray contrast media (XRC) by ozonation in a complex wastewater matrix–urine as example, *Water Science and Technology*, **55**, 293-300.

Haiß A., and Kümmerer K. (2006), Biodegradability of the X-ray contrast compound diatrizoic acid, identification of aerobic degradation products and effects against sewage sludge micro-organisms, *Chemosphere*, **62**, 294-302.

Hapeshi E., Lambrianides A., Koutsoftas P., Kastanos E., Michael C., and Fatta-Kassinos D. (2013), Investigating the fate of iodinated X-ray contrast media iohexol and diatrizoate during microbial degradation in an MBBR system treating urban wastewater, *Environmental Science and Pollution Research*, **20**, 3592-3606.

Hashimoto K., Irie H., and Fujishima A. (2005), TiO$_2$ photocatalysis: a historical overview and future prospects. *Japanese Journal of Applied Physics*, **44**, 8269.

Kalsch W. (1999), Biodegradation of the iodinated X-ray contrast media diatrizoate and iopromide, *Science of the Total Environment*, **225**, 143-153.

Kerkez Ö., and Boz İ. (2015), Photodegradation of methylene blue with Ag$_2$O/TiO$_2$ under visible light: operational parameters, *Chemical Engineering Communications*, 202, 534-541.

Kormos J.L., Schulz M., and Ternes T.A. (2011), Occurrence of iodinated X-ray contrast media and their biotransformation products in the urban water cycle, *Environmental Science and Technology*, **45**, 8723-8732.

Kormos J.L., Schulz M., and Ternes, T.A. (2011), Occurrence of iodinated X-ray contrast media and their biotransformation products in the urban water cycle, *Environmental Science & Technology*, **45**, 8723-8732.

Li G., Dimitrijevic N.M., Chen L., Rajh T., and Gray K.A. (2008), Role of surface/interfacial Cu^{2+} sites in the photocatalytic activity of coupled CuO$^-$ TiO$_2$ nanocomposites, *The Journal of Physical Chemistry C*, **112**, 19040-19044.

Oros-Ruiz S., Zanella R., and Prado B. (2013), Photocatalytic degradation of trimethoprim by metallic nanoparticles supported on TiO$_2$-P25. *Journal of Hazardous Materials*, **263**, 28-35.

Oros-Ruiz S., Zanella R., López R., Hernández-Gordillo A., and Gómez R. (2013), Photocatalytic hydrogen production by water/methanol decomposition using Au/TiO$_2$ prepared by

deposition–precipitation with urea. *Journal of Hazardous Materials*, **263**, 2-10.

Pérez S., and Barceló D. (2007), Fate and occurrence of X-ray contrast media in the environment, *Analytical and Bioanalytical Chemistry*, **387**, 1235-1246.

Putschew A., Wischnack S., and Jekel M. (2000), Occurrence of triiodinated X-ray contrast agents in the aquatic environment, *Science of the Total Environment*, **255**, 129-134.

Qin S., Xin F., Liu Y., Yin X., and Ma W. (2011), Photocatalytic reduction of CO_2 in methanol to methyl formate over CuO–TiO_2 composite catalysts, *Journal of Colloid and Interface Science*, **356**, 257-261.

Schittko S., Putschew A., and Jekel M. (2004), Bank filtration: a suitable process for the removal of iodinated X-ray contrast media?, *Water Science and Technology*, **50**, 261-268.

Schulz M., Löffler D., Wagner M., and Ternes T.A. (2008), Transformation of the X-ray contrast medium iopromide in soil and biological wastewater treatment. *Environmental Science and Technology*, **42**, 7207-7217.

Seitz W., Weber W.H., Jiang J.Q., Lloyd B.J., Maier M., Maier D., and Schulz W. (2006), Monitoring of iodinated X-ray contrast media in surface water, *Chemosphere*, **64**, 1318-1324.

Steger-Hartmann T., Länge R., Schweinfurth H., Tschampel M., and Rehmann I. (2002), Investigations into the environmental fate and effects of iopromide (ultravist), a widely used iodinated X-ray contrast medium, *Water Research*, **36**, 266-274.

Sugihara M.N., Moeller D., Paul T., and Strathmann T.J. (2013), TiO_2-photocatalyzed transformation of the recalcitrant X-ray contrast agent diatrizoate, *Applied Catalysis B: Environmental*, **129**, 114-122.

Ternes T.A., Stüber J., Herrmann N., McDowell D., Ried A., Kampmann M., and Teiser, B. (2003), Ozonation: a tool for removal of pharmaceuticals, contrast media and musk fragrances from wastewater?, *Water Research*, **37**, 1976-1982.

Wang X., Li S., Yu H., Yu J., and Liu S. (2011), Ag_2O as a new visible-light photocatalyst: Self-stability and high photocatalytic activity, *Chemistry-A European Journal*, **17**, 7777-7780.

Weissbrodt D., Kovalova L., Ort C., Pazhepurackel V., Moser R., Hollender J., Seigrist, H., and McArdell C.S. (2009), Mass flows of X-ray contrast media and cytostatics in hospital wastewater, *Environmental Science and Technology*, **43**, 4810-4817.

Zhao C., Arroyo-Mora L.E., DeCaprio, A.P., Sharma V.K., Dionysiou D.D., and O'Shea K.E. (2014), Reductive and oxidative degradation of iopamidol, iodinated X-ray contrast media, by Fe (III)-oxalate under UV and visible light treatment, *Water Research*, **67**, 144-153.

Zhou W., Liu H., Wang J., Liu D., Du G., and Cui J. (2010),, Ag_2O/TiO_2 nanobelts heterostructure with enhanced ultraviolet and visible photocatalytic activity, *ACS Applied Materials and Interfaces*, **2**, 2385-2392.